iScience, Volume *23*

Supplemental Information

Origin and Lineage Plasticity of Endogenous Lacrimal Gland Epithelial Stem/Progenitor Cells

Liana Basova, Geraint J. Parfitt, Alex Richardson, Vanessa Delcroix, Takeshi Umazume, Daniel Pelaez, David T. Tse, Ivo Kalajzic, Nick Di Girolamo, James V. Jester, and Helen P. Makarenkova

SUPPLEMENTAL INFORMATION

SUPPLEMENTAL FIGURES

Figure S1. *Analysis of GFP expression in the LG of unchased and chased H2B-GFP/K5tTA and mice. Related to figure 1.* (A-E') H2B-GFP/K5tTA mice were pulsed from P0 to P28 to label all cytokeratin 5^+ epithelial cells with nuclear green fluorescence protein (GFP). At P28, H2B-GFP/K5tTA mice were sacrificed and the LGs or frozen sections of glands were immunostained with anti-αSMA and analyzed for GFP expression. (A, C) Almost all MECs exhibited nuclear GFP; however, we also identified a small percentage of unlabeled MECs (B, white arrows). (C) Almost all cells of intercalated ducts labeled with GFP. (D) Example of excretory ducts in unchased LGs showing labeling in basal ductal cells (*BD* - white arrows). αSMA staining (red) detects pericytes in the blood vessels (D, red arrows). (E) Quantification of GFP expressing cells in different LG compartments. Approximately 35 randomly taken sections of approximately 10 mm length and 6 mm width and 5-7 fields of each section have been analyzed (MEC - myoepithelial cells, BD -basal ductal cells, ID – intercalated duct cells, LUM – luminal ductal cells, AC acinar cells). (E') An example of excretory duct (*ED*) image, showing a couple of labeled luminal cells (white arrows). This particular image was equalized using Photoshop, which allows to see the ductal cell shape. Note: Only a low percentage of labeled luminal cells were detected. (F-H) The H2B-GFP/K5tTA mice were pulsed from P0 to P28 to label proliferating cells. At P28, H2B-GFP/K5tTA mice were fed a doxycycline-containing diet for 8 weeks (chase) and frozen sections of the LGs obtained from these mice were immunostained with the Krt5 (F) or Krt14 (G and H, grey) and αSMA (G, red) to visualize basal ductal cells and MECs. No GFP was found in the acinar and luminal compartments. LRCs (green) are found in a subset of basal ductal cells expressing Krt5/Krt14 but not in MECs (G, *MEC*, red arrows). (I -K) Distal embryonic LG bud marker Sox10 (Chen et al., 2014) continues to be expressed in the distal epithelial structures (acinar and MEC cells) of the LG during early postnatal development (I and J) and adulthood (K, MECs - white arrows), but not in the ducts (*duct*).

Fifure S2. *Single channel images of Figure 1E. Related to Figure 1E.* (E') – DAPI; (E'') - GFP (LRCs). (E''') – Immunostaining for αSMA, (E'''') – immunostaining for c-kit.

Figure S3. *Single channel images of Figure 1F. Related to Figure 1F.* (F') – DAPI; (F'') - GFP (LRCs). (F''') – Immunostaining for αSMA, (F'''') – immunostaining for Krt14.

Figure S4 *Expression pattern of Krt5 and 14 in the LG. Related to Figure 2.* (A-D) Section of LG stained with Krt15 (green) Krt5 (pink) and αSMA (red) antibodies. (E-H) Immunostatining of LG lobule with Krt14 (red) and Krt5 (green) antibodies. Note: no acinar cells are labeled. (I-L) immunostaining of the LG at E19.5 with Krt14 (green) and Krt5 (red antibodies) showing labeling of basal layer of ducts. Nuclei labeled with DAPI. Although expression pattern of Krt5 and Krt14 was not completely overlapped (especially in MECs: (A, B, D and E-H) both keratins were found only within two compartments of the LG: MEC and basal ductal.

Figure S5. *Single channel images and DAPI of Figure 2C. Related to Figure 2C.* (C') Krt14 (dsRed) + DAPI; (C'') – Krt14 (GFP) +DAPI; (C''') - Immunostaining for αSMA (Orange) + DAPI, (C'''') – merged image. Scale bar is 8 μm.

Figure S6. *Apical parts of luminal cells and basal ductal cells show a high level of filamentous actin. Related to Figure 2.* (A, B) Rhodamine-phalloidin staining reveals filamentous actin in the apical part (*ap*) of the luminal ductal cells and in a subset of basal ductal cells (white arrows).

Figure S7. *IL1α injection induces severe damage of the LG acinar compartment. Related to Figure 6.* (A, B) LG structure 1 day after IL1α injection. Majority of acinar cells in IL1α injected LG lobules are destroyed. Acini left after IL1α injection are labeled by black arrows. Some acinar cells become dense, thus suggesting degeneration (red arrows). (C, D) LG structure 3 days after injury. Number of infiltrating cells decreases, and small regenerating acini appear (D, white arrowheads). (E) Control LG injected with vehicle (saline) (one day after injection) has normal structure. Paraffin sections of IL1α and saline injected LGs were stained with fast red. LGs were obtained from female mice.

Figure S8. *Expression of ductal and MEC markers in human lacrimal gland (HLG). Related to figure 8.* Frozen sections were stained with the Krt5 (basal ductal and MEC marker), Krt14 (basal ductal and MEC

marker), Krt19 (luminal ductal marker) and SMA (MEC marker) antibodies. As expected, both Krt14 (A-C) and Krt5 (D-F) labeled ductal and MEC cells. Ductal marker Krt19 (G-I) labeled luminal cells and was not expressed in MECs. Abbreviation: *ac* - acini.

Figure S9. *Progression of lineage restriction with LG maturation. Related to Figure 9.* During embryonic development LG epithelium contains multipotent stem/progenitor cells able to give rise to several cell lineages. At the same time αSMA^{+} MEC lineage becomes restricted early in embryonic development. (B) Following birth, lineages become established and the fate of progenitor cell descendants becomes restricted.

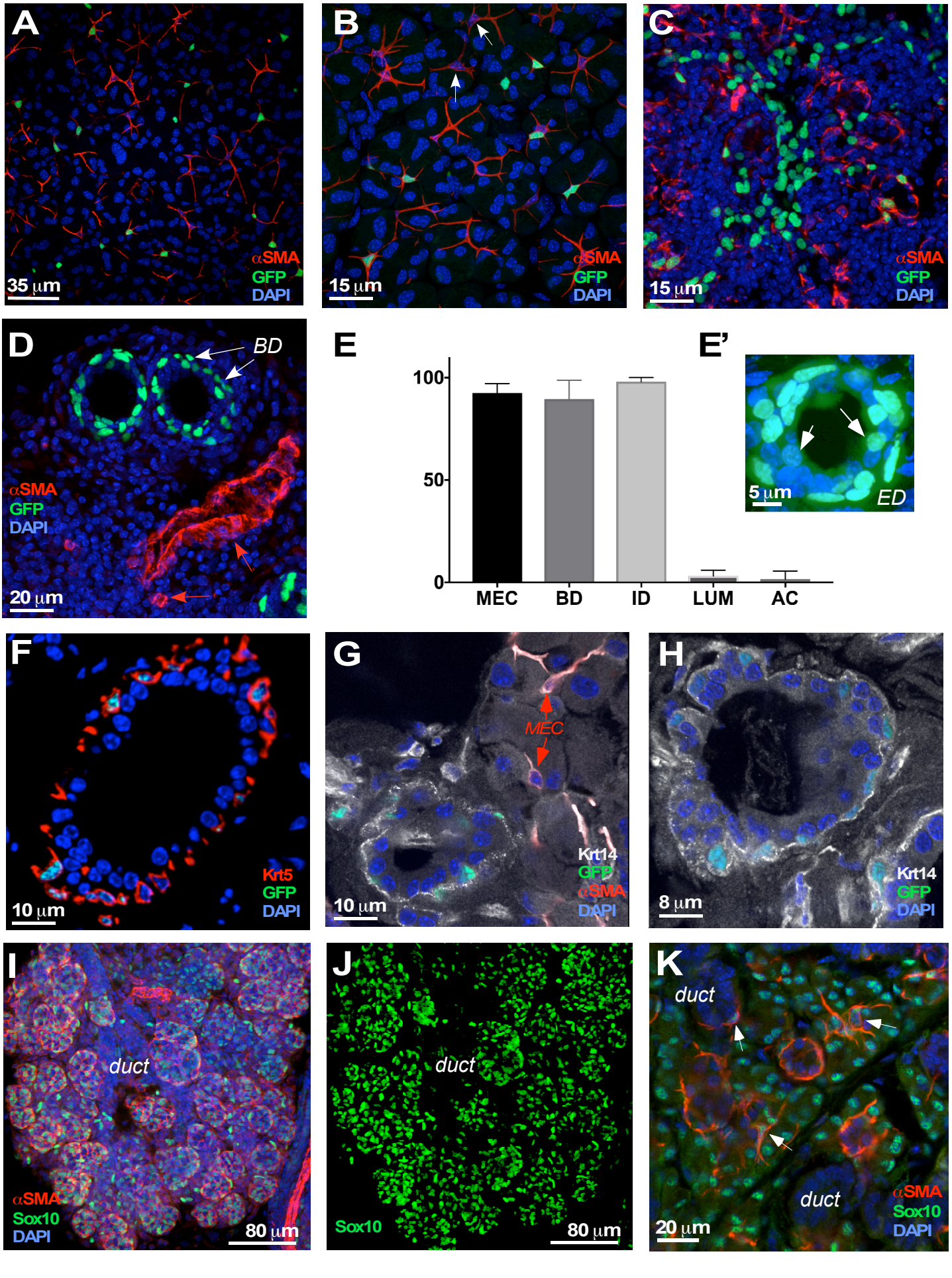

Figure S 1, related to Figure 1.

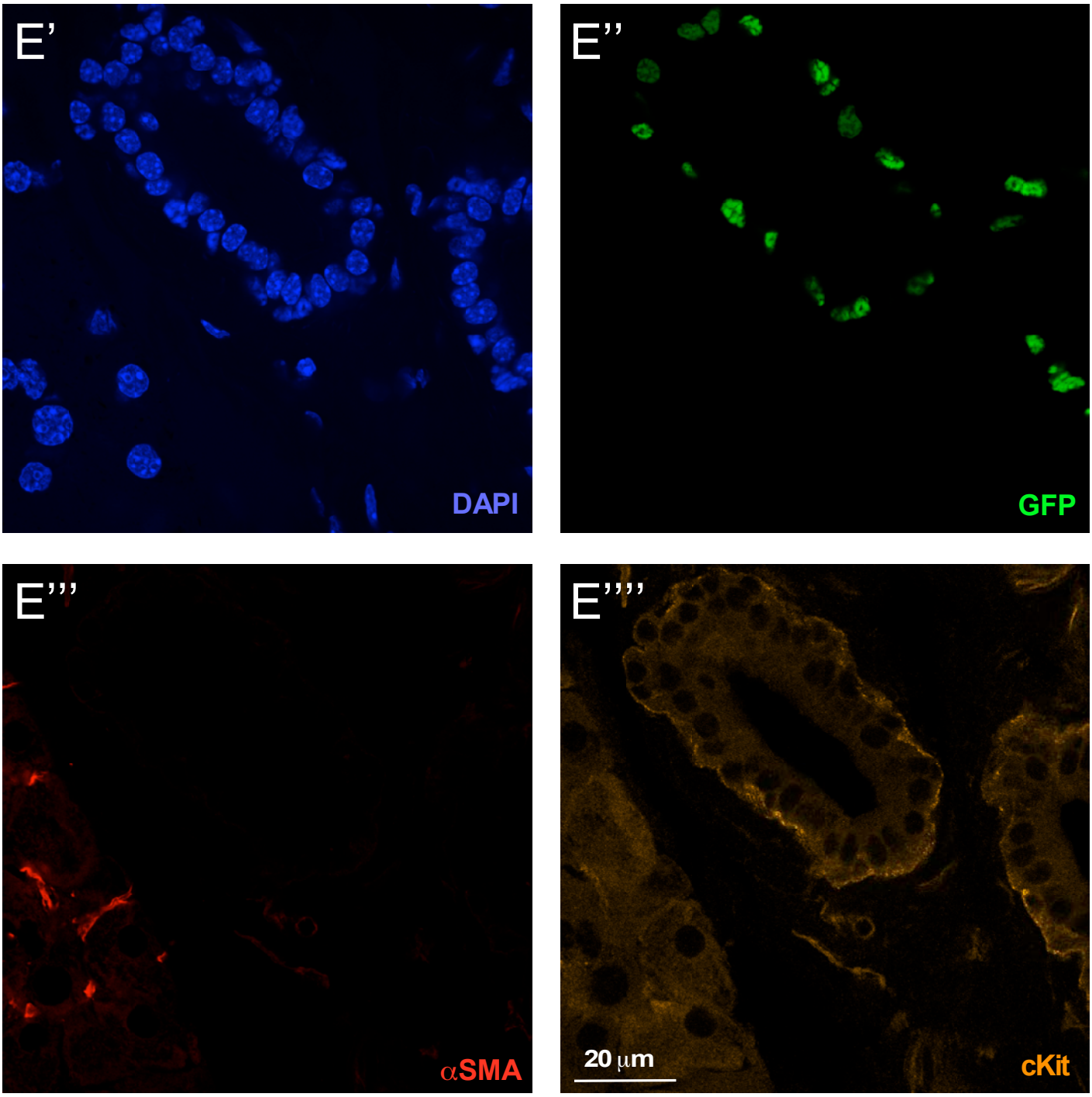

Figure S2, related to Figure 1E.

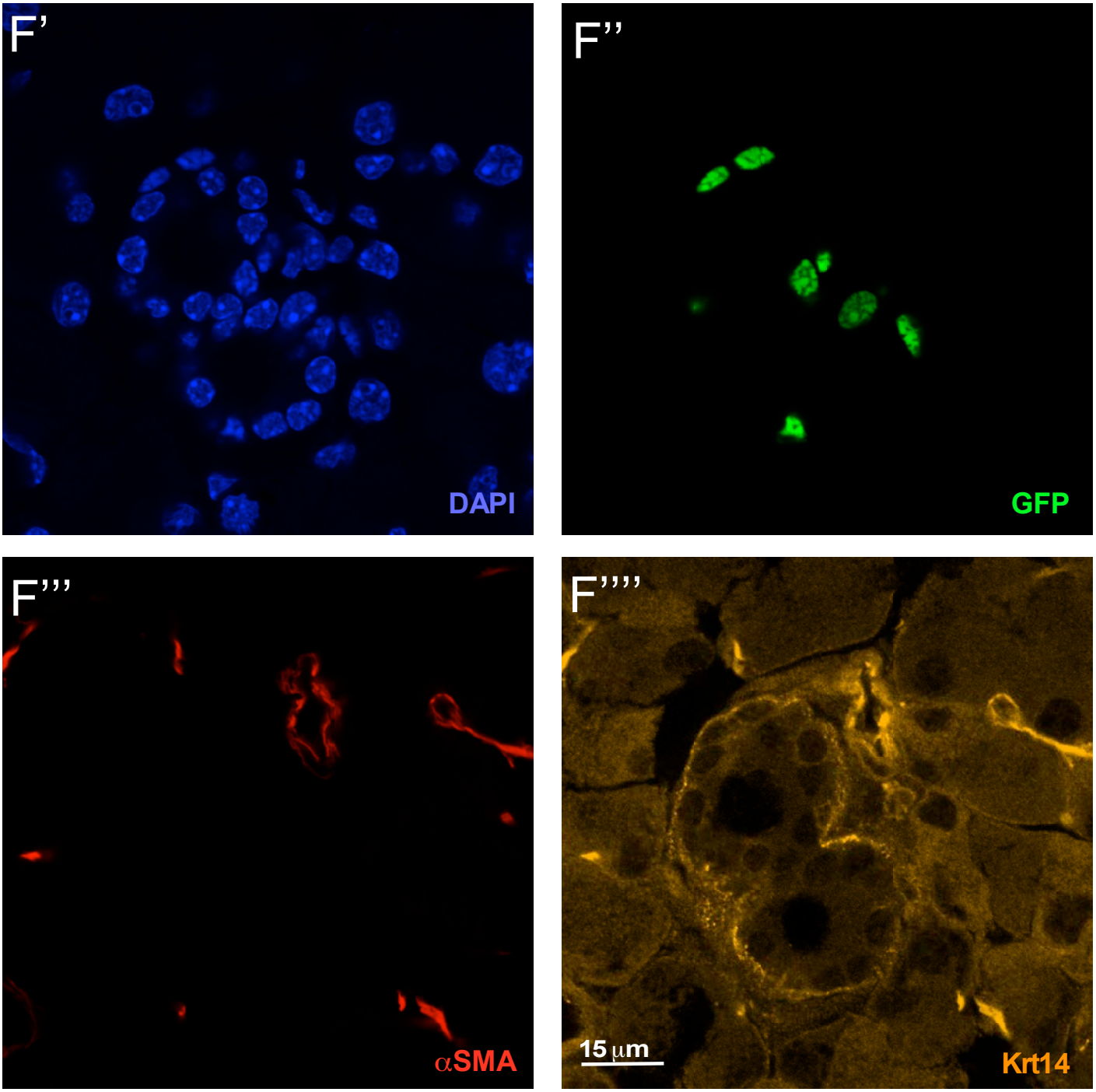

Figure S3 Related to figure 1F.

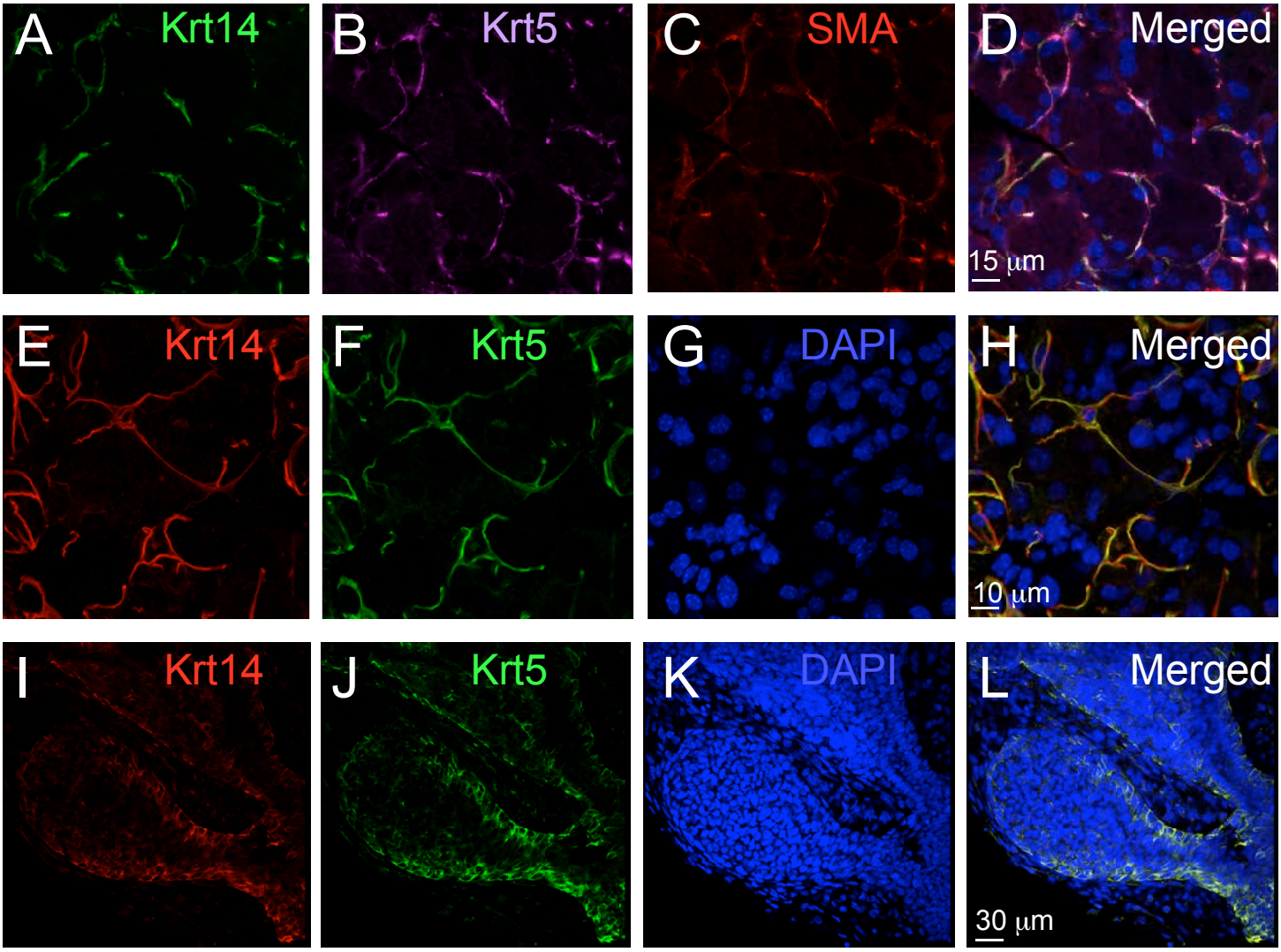

Figure S4, Related to Figure 2.

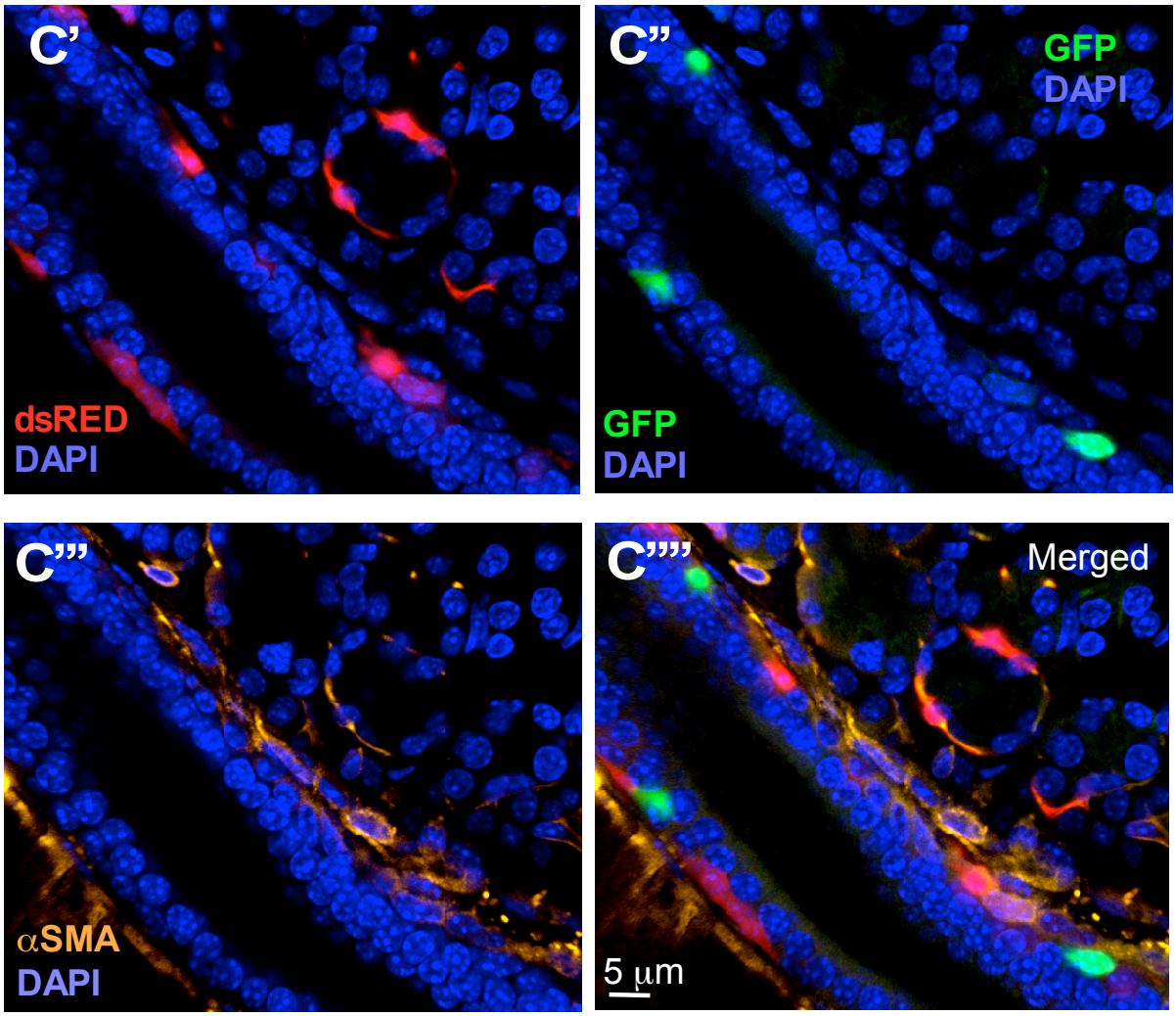

Figure S5, related to Figure 2C.

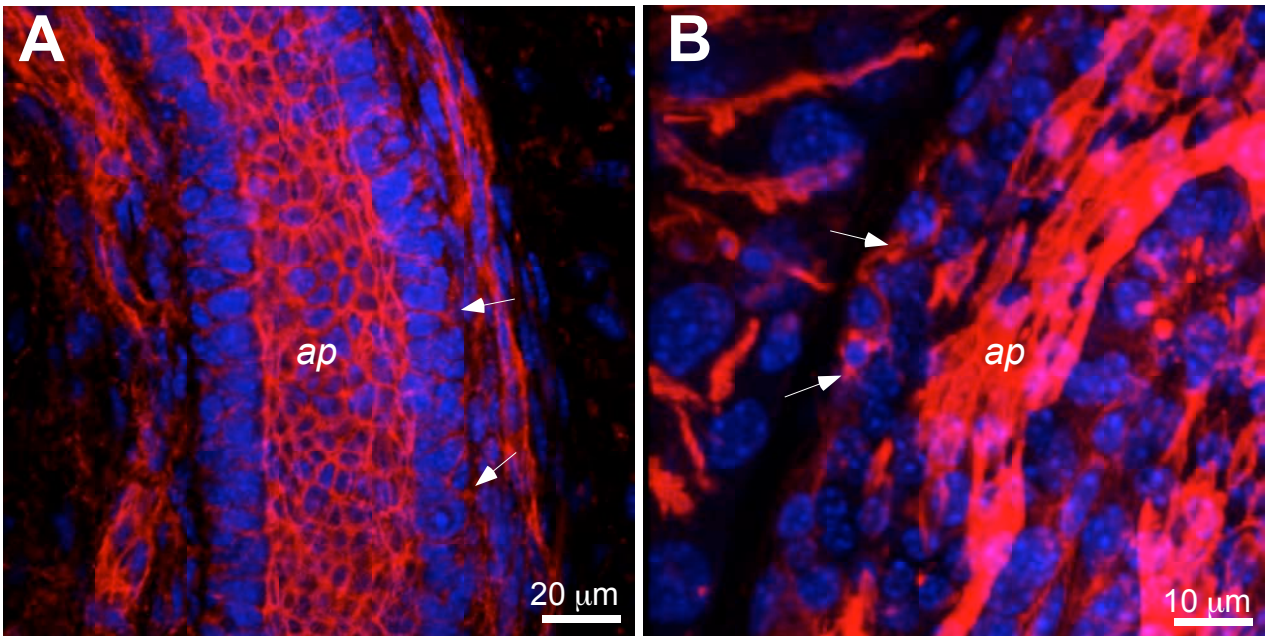

Figure S6, related to Figure 2.

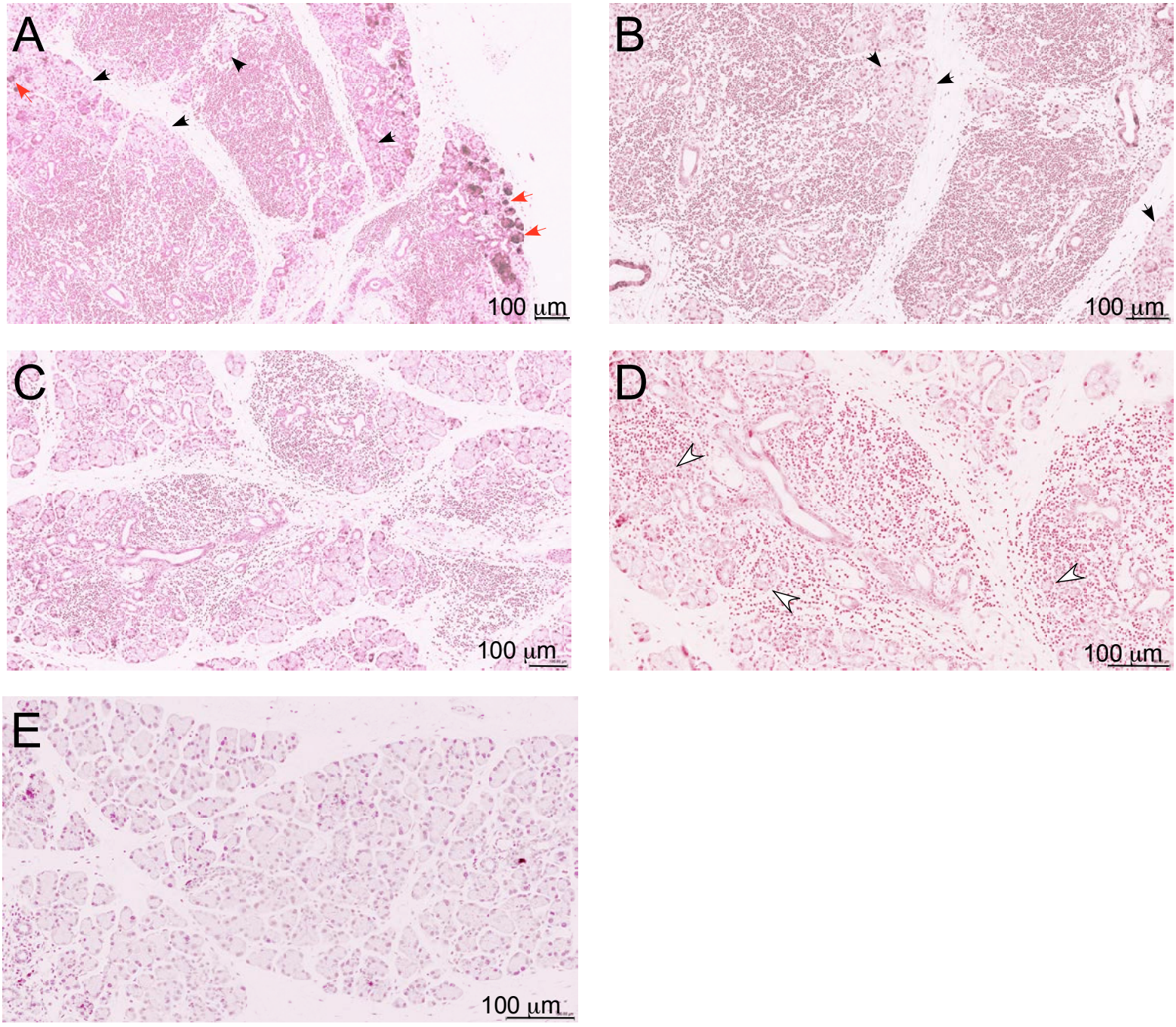

Figure S7, related to Figure 6.

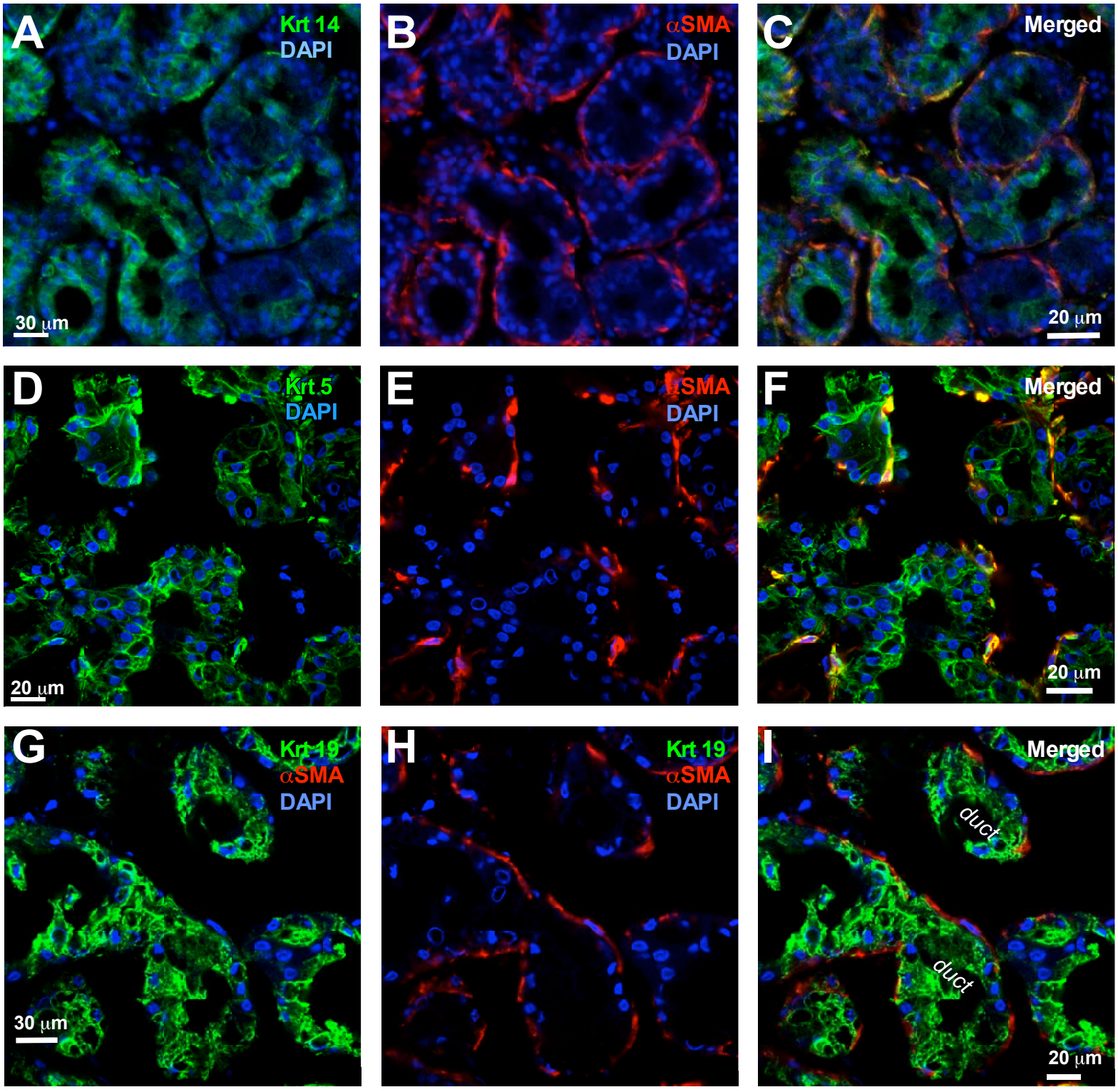

Figure S8, related to Figure 8.

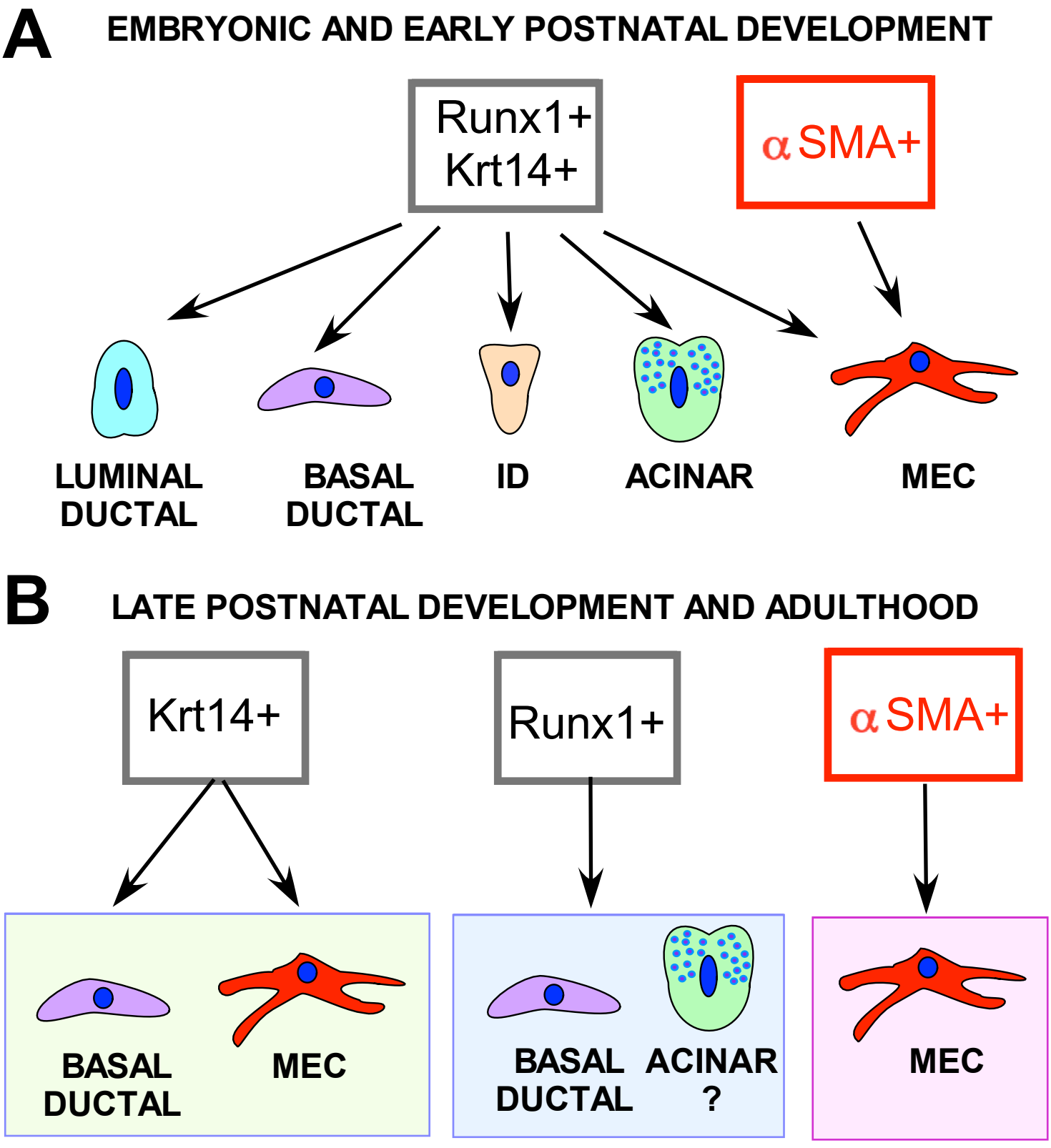

Figure S9, related to Figure 9.

Table S1. Key Reagents and Resources (Related to Figures 1-8, S1-S8 and Transparent Methods)

REAGENT/RESOURSE	SOURCE	IDENTIFIER
Chemicals, kits and recombinant proteins		
4′,6-diamidino-2-phenylindole (DAPI)	Millipore/Sigma	32670
Tamoxifen	Millipore/Sigma	T5648
Progesterone	Millipore/Sigma	P3972
UltraPure™ Low Melting Point Agarose	ThermoFisher Scientific	16520050
Ethanol, Absolute (200 Proof), Molecular Biology Grade	Fisher Scientific	BP 2818,
Xylene (Certified ACS)	Fisher Scientific	X5-500
PBS, Phosphate Buffered Saline, 10X Solution	Fisher Scientific	BP 39920
Sodium Citrate dihydrate (mw: 294.1 g/mol)	Millipore/Sigma	W302600
Citric Acid (mw: 192.1 g/mol)	Millipore/Sigma	251275
DPBS, no calcium, no magnesium	ThermoFisher Scientific	14190144
Gelatin from bovine skin	Millipore/Sigma	G9391
Goat serum	Millipore/Sigma	G9023
2-Methylbutane	Millipore/Sigma	277258
Paraformaldehyde, granular, EM Grade, purified	WVR	100504-160
Tris base	Millipore/Sigma	T1503
Hydrochloric acid	Millipore/Sigma	H1758
Sodium chloride	Millipore/Sigma	1064001000
Sodium hydroxide	Millipore/Sigma	S8045
Flash Phalloidin™ Red 594	Bio-Legend	424203
Fluorescence Mounting Medium	DAKO	S302380
IgG from rabbit serum	Millipore/Sigma	I5006
IgG from mouse serum	Millipore/Sigma	I5381
IgG from goat serum	Millipore/Sigma	I5256
CytoVista Tissue Clearing Reagent	ThermoFisher Scientific	V11300
TWEEN® 20	Millipore/Sigma	P1379
Sodium Chloride 0.9% (Normal Saline), USP, Sterile Grade	Fisher Scientific	Z1376
Hydrogen Peroxide, 30% (Certified ACS)	Fisher Scientific	H325
Methanol (Certified ACS)	Fisher Scientific	A412
Richard-Allan Scientific™ Cytoseal™ XYL	ThermoFisher Scientific	8312-4
Fisherbrand™ Cover Glasses: Rectangles	Fisher Scientific	12-545-M
Thimerosal	Millipore/Sigma	T5125
Casein from bovine milk	Millipore/Sigma	C5890
Phosphate buffered saline	Millipore/Sigma	P4417
Gill Hematoxylin Stain	Fisher Scientific	CS400-1D
VECTASTAIN® Elite ABC-HRP Kit (Peroxidase, Universal)	Vector Laboratories	PK-6200

Vector® NovaRED® Substrate Kit, Peroxidase (HRP)	Vector Laboratories	SK-4800
Tissue-Plus™ O.C.T. Compound	Fisher Scientific	23-730-571
Recombinant Human IL-1 alpha	R&D systems	200-LA-010
Methyl methacrylate	Polysciences	00834.
Butryl methacrylate	Millipore/Sigma	235865
Software		
ImageJ	NIH	N/A
MetaMorph	BioVision technologies	N/A
Prizm 7	GraphPad Software	N/A
Excel	Microsoft	N/A
IMARIS	Oxford Instruments	N/A

Table S2. Primary antibody used for immunoassaying of whole mount preparations and/or frozen, paraffin, plastic sections (Related to Figures 1-6, 8, S1-S5, S8 and Transparent Methods)

Antibody	Antibody information	Whole mount and frozen sections	Paraffin, plastic sections
Sox9 (rabbit monoclonal)	Millipore/Sigma clone 2B10, cat# ZRB5535 (IgG)		1:50
Sox9 (rabbit monoclonal)	Abcam, clone EPR14335-78, cat# ab185966 (IgG)	1:100	1:20
αSMA (mouse monoclonal)	Clone 1A4, ascites fluid, cat# A2547 (IgG2a)	1:400	1:100
RFP (rabbit polyclonal)	Thermo Fisher Scientific, cat# R10367	-	1:1000
Sox10 (goat polyclonal)	Santa Cruz Biotechnology, (N20) Cat# sc-17342	1:100	1:20
Cytokeratin 5 (Krt5) (rabbit monoclonal)	Abcam, clone EP1601Y, cat# ab52635 (IgG)	1:100	1:50
Cytokeratin 5 (Krt5) (mouse monoclonal)	ThermoFisher Scientific, clone 2C2 MA517057 (IgG1)	1:100	
Cytokeratin 14 (Krt14) (mouse monoclonal)	Abcam, clone LL002, cat# ab7800 (IgG3)	1:100	1:50
Cytokeratin 14 antibody, (rabbit monoclonal)	Millipore/Sigma, clone SP53, SAB5500124	1:100	
Thrombospondin 1 (Thbs1) (goat polyclonal)	Santa Cruz Biotechnology Inc., (N-20) cat# sc-12312		1:50
Panx1 (rabbit polyclonal)	Millipore/Sigma, cat# HPA016930	1:100	
Claudin-1 (mouse monoclonal)	Thermo Fisher Scientific, clone 2H10D10, cat# 37-4900 (IgG1)	1:100	
Pax-6 (rabbit polyclonal)	BioLegend, cat# 901301 (previously Covance, cat# PRB-278P)	1:100	
Ser28 phosphorylated histone H3 (rat monoclonal)	Millipore/Sigma, clone HTA28, cat# H9908 (IgG2a)	1:200	

Transparent Materials and Methods

1. Mouse strains and breeding

All experiments were carried out in accordance with the ARVO statement for the Use of Animals in Ophthalmic and Vision Research and were approved by the Scripps Research Institute and the Gavin Herbert Eye Institute Animal Care and Use Committees.

H2B-GFP (Also known as: pTRE-H2BGFP) mice are commercially available from Jackson Laboratories (stock number: 005104) and K5tTA mice were kindly provided by Adam Glick (Diamond et al., 2000). H2B-GFP/K5tTA mice on an FVB background were genotyped and pulsed from P0 to P28 to label all cytokeratin 5^{+} epithelial cells with nuclear green fluorescence protein (GFP). At P28, H2B-GFP/K5tTA mice were fed a doxycycline-containing diet (2g/kg) to initiate the chase period. Krt5^{+} epithelial cells lose 50% of their GFP intensity with every division and quiescent cells retain their GFP label (Parfitt et. al. 2015).

Several mouse lines were used for lineage tracing experiments. Mice expressing tamoxifen (TM)-inducible Cre under control of α-smooth muscle actin (SMA^{CreERT2}) generated by Dr. Kalajzic (Grcevic et al., 2012). αSMA^{CreERT2} mice were crossed with reporter lines, Rosa26-Confetti (Stock No. 017492) and Rosa 26-tdTomato (Stock No 007909, also known as Ai9 (RCL-tdT)) to generate Sma$^{CreERT2/+}$:Rosa26-Confetti$^{fl/+}$ and Sma$^{CreERT2/+}$:Rosa26-tdTomato$^{fl/fl}$. Mice were injected with TM on two consecutive days during embryonic, early postnatal development or adulthood and analyzed following various time periods. Rosa26-Confetti mice were obtained from Jackson Labs.

To study Krt14 cell lineage in the LG, Krt14 $^{CreERT2/+}$:Rosa26-Confetti$^{fl/+}$ mice were injected with TM at the embryonic day 15 (E 15), at one week of postnatal development (P7), six weeks (P36) and ten weeks (P74) of age as previously described (Di Girolamo et al., 2015; Richardson et al., 2017) and tissue from these mice was resected and analyzed at two (P14), four (P30), eight (P60), twenty (P140), and thirty (P210) weeks of age.

A TM-inducible Cre line under the control of the Runx1 promoter (Runx1$^{Mer\text{-}Cre\text{-}Mer/+}$) was generated and generously provided by Dr. Samokhvalov (Samokhvalov et al., 2007) and the RIKEN Center for Life Science Technologies (CLST). This mouse line was used to generate the Runx1$^{Mer\text{-}Cre\text{-}Mer/+}$:Rosa26-Confetti$^{fl/+}$ line.

All Confetti reporter mouse lines used in this study contained the Brainbow 2.1 fluorescent multicolor reporter cassette. All control mice including the TM-inducible reporter mice with no TM injection showed no ectopic cell labeling.

Males and females did not show difference in cell labeling and distribution.

2. Tamoxifen preparation and administration and analysis of clones

Tamoxifen (TM: 1 g) (cat# T5648-1G, Sigma) (also see Table S1 for all reagents and resources) was dissociated in ethanol (2ml) and diluted in filtered corn oil to a final concentration of TM was 20 mg/ml. The solution was vortexed and placed on shaker at 45°C overnight. When completely dissolved, aliquots were stored at -80ºC. TM (1-2 mg/20 g body weight) was administered on 2 consecutive days to adult mice by intraperitoneal injection and to pups by oral gavage.

To label cells during embryonic development TM was administrated by IP to pregnant females at desired times. To neutralize the partial estrogen receptor agonist effects of tamoxifen, which can result in fetal abortions, progesterone (cat# P3972, Millipore/Sigma) (also dissolved in corn oil) was added (at half the total TM dose given, up to 1.5-2 mg of progesterone for single injection). Generally, a single dose of TM 1.5–3 mg was enough to induce reporter expression.

A clone was identified as containing one or several cells with only single fluorescent color. Labeled cells were identified by DAPI staining labeling induced in Rosa26-Confetti reporter mouse by a specific Cre-driver. Ten to twenty random areas (depending on gland size) within each gland were chosen for analysis, from at least three-five biological replicates. Clone sizes of RFP (red cytoplasmic, GFP (green, nuclear), YFP (pale green cytoplasmic), and CFP (blue membrane) labeled cells were analyzed using IMARIS. An average we we able to identify around 100-150 separate clones per gland at each timepoint. Clonal analysis was performed separately within each cellular compartment.

3. Butyl-methyl methacrylate embedding of lacrimal glands

LGs dissected from H2B-GFP/K5tTA mice were immediately fixed in 4% paraformaldehyde (PFA) on ice for plastic embedding. $K14^{CreERT2}$:Confetti mouse lacrimal glands were fixed in 4% PFA up to 59 weeks after TM-induced labeling (69 weeks of age). After fixation, tissues were embedded in 3% low-melting point agarose and dehydrated in 50%, 75%, 95% and then 100% ethanol for 30 minutes each. Butyl-methyl methacrylate (BMMA: Butyl methacrylate, cat# 235865, Millipore/Sigma, St. Louis, MO; Methyl methacrylate, cat# 00834, Polysciences , Warrington, PA) resin infiltration was carried out sequentially in ethanol:BMMA at 2:1, 1:1 and 1:2 ratios for >12 hrs each at 4°C. BMMA-embedded tissues were polymerized under UV light at 4°C for 8 hrs to obtain a plastic block for serial sectioning (Parfitt, 2019).

4. Primary antibodies

The following primary antibodies (Table S2)were used for immunostaining: Sox9 rabbit monoclonal, Sox10 goat polyclonal (N-20), mouse monoclonal α-SMA, Cytokeratin 5 (Krt5) rabbit monoclonal, Cytokeratin 14 (Krt14) mouse monoclonal, and Thrombospondin 1 (Thbs1) goat polyclonal antibody (N-20), Panx1 rabbit polyclonal, Claudin-1 mouse monoclonal), Pax6 rabbit polyclonal, Ser28 phosphorylated histone H3 rat monoclonal, RFP rabbit polyclonal.

5. Immunostaining of BMMA plastic serial-sections

BMMA-embedded lacrimal glands were serially sectioned at 2 µm using a diamond knife attached to an Ultra-microtome (Leica), and the ribbons of sequential serial sections (20 sections/ribbon) were mounted onto 5% gelatin coated slides (2 ribbons/slide) and dried using a slide heater set to 55°C. Slides were then immersed in acetone for 10 mins at room temperature before being rehydrated in 95%, 75% and 50% ethanol. Antigen retrieval was performed for 7 minutes using 1X Sodium Citrate buffer (pH 6.0) in a pressure cooker. After blocking in 5% goat serum, sections were immuno-stained overnight at 4°C with primary antibodies, including anti-RFP to retrieve endogenous fluorescence lost due to ethanol dehydration, Sox9 and αSMA. Tissue sections were then incubated with appropriate secondary antibodies including (Invitrogen) at 37°C for 1 hr.

6. 3-D reconstruction (Immuno-fluorescence tomography)

Fluorescence imaging of serial sections was conducted on a Leica DMI6000B microscope with MetaMorph software for multi-dimensional, mosaic image acquisition. LGs were imaged for GFP before immunostaining was performed to preserve the signal. Mosaic imaging of 3x3 tiles was performed for each section and images were acquired at a pixel resolution of 0.44 µm x 0.44 µm x 2 µm using a 20X/0.75NA objective. Mosaic images of each section were compiled into image stacks using ImageJ software before alignment and 3-D reconstruction using Amira 4.6. The average pixel intensities of GFP+ LRCs was calculated using Amira segmentation software and each LRC was assigned into a category based on their intensity value and level of label retention, with the LRC+++ subpopulation being the most quiescent i.e., LRC+ = 0–100; LRC++ = 100–200; LRC+++ = 200–255. Quantification of total cells and fluorescence intensity of LRCs was carried out using ImageJ's 3-D objects counter.

7. Immunostaining and confocal microscopy

Alternatively LGs dissected from reporter mice (Confetti and Tomato) were fixed with 2% PFA in PBS (pH 7.4) for 20-40 minutes and processed for whole mount immunostaining (see below) or frozen in 2-methylbutane (isopentane; Sigma-Aldrich, St. Louis, MO, USA) cooled by liquid nitrogen, and 15 µm sections were cut with a Microm HM500 cryostat (MICROM International GmbH, Dreieich, Germany). Sections were blocked with 5% goat serum in Tris-buffered saline containing 0.1% Tween 20 (TBST) then incubated with respective primary antibodies at 4°C overnight. Appropriate secondary antibodies were purchased from Thermo Fisher Scientific (Molecular Probes, Waltham, MA). Images were taken using a Zeiss LSM 780 laser scanning confocal microscope (LSCM). The isotype-specific immunoglobulins (normal human, rabbit, goat or mouse IgGs; Millipore/Sigma) or pre-immune serum were used for negative controls. Flash Phalloidin™ Red 594 (Bio-Legend, cat# 424203) has been used to visualize F-actin filaments.

8. Whole mount immunostatining

Permeabilized LG (see above) were separated into lobules and stained with primary antibodies (Table S2) overnight washed 3-4 times with Tris-buffered saline pH 7.5 with 0.1% Tween 20 (TBST) and stained with secondary antibodies for 45-60 mins at room temperature (RT). Where appropriate, nuclei were counter-stained with DAPI. When necessary a CytoVista Tissue Clearing Reagent (V11300, ThermoFisher) has been used for 3D fluorescent imaging of large pieces of LG.

9. Lacrimal gland injury experiments

Female $Sma^{CreERT2/+}$:Rosa26-$tdTomato^{fl/fl}$ mice were injected with TM at P28-30 or at P58-60 to label MECs and ten days later animals were anesthetized, shaved, and control lacrimal glands were injected with vehicle (saline) or were injected with recombinant human interleukin IL-1α (1 µg dissolved in 2 µl of saline), as previously described (Zoukhri et al., 2008). To ensure that the LG is efficiently injured several injections into different LG lobules of each gland were done. Two weeks later, the animals were sacrificed, and the lacrimal glands were dissected and analyzed.

10. Immunohistochemistry on human LG paraffin sections

Human LGs from three donors (all donors were female donors aged 62, 84, and 90 years old) were obtained from Advanced Tissue Services (Phoenix, AZ, USA) or from one of the coauthors (DTT). Tissues were fixed immediately and embedded in paraffin in Scripps histology core facility or processed for frozen sectioning (see above), and 5 µm sections were prepared. Endogenous peroxidase activity on rehydrated sections was blocked by treating slides with 3% hydrogen peroxide in absolute methanol for 30 mins. Antigen retrieval was performed for 40 mins using 0.01 M citrate (pH 6.0) in a humidified heated chamber. Sections were blocked with 5 g/L casein in PBS containing 0.5 g/L thimerosal (Sigma-Aldrich; cat# T5125-25G) for 30 minutes, incubated with primary antibodies, and diluted in casein buffer overnight at 4°C. Sox10, Sox9, Krt5, Krt14, α-SMA, and Thbs1 primary antibodies were used for immunostaining (Table S2). Biotinylated secondary antibodies (Vector Labs, Burlingame, CA) were used at a 1:300 dilution. Visualization was achieved using biotin/avidin-peroxidase (Vector Labs) and Nova Red (Vector Labs). Tissue was counterstained with Gill's hematoxylin (Fisher Scientific, San Diego, CA; CS400).

11. Statistical Analysis and Data Presentation

For experiments using animals, animal numbers reflect group sizes. For non-animal experiments values of n reflect the number of independent experiments performed or number of LG analyzed. Statistical analyses were performed with Prism version 7.00 for Windows (GraphPad Software, La Jolla, CA; www.graphpad.com) or with Excel (Microsoft). Histograms are presented as mean ± SD from a representative experiment or of the normalized data from several experiments. Statistical analysis was performed with unpaired two-tailed Student's *t*-test and two-tailed Fisher's exact tests and a p-value <0.05 was considered statistically significant. Clonal analysis was performed using one-way ANOVA or using Wilcoxon Signed Paired Rank Test.

Supplemental References

Chen, Z., Huang, J., Liu, Y., Dattilo, L.K., Huh, S.H., Ornitz, D., and Beebe, D.C. (2014). FGF signaling activates a Sox9-Sox10 pathway for the formation and branching morphogenesis of mouse ocular glands. Development *141*, 2691-2701.

Di Girolamo, N., Bobba, S., Raviraj, V., Delic, N.C., Slapetova, I., Nicovich, P.R., Halliday, G.M., Wakefield, D., Whan, R., and Lyons, J.G. (2015). Tracing the fate of limbal epithelial progenitor cells in the murine cornea. Stem cells (Dayton, Ohio) *33*, 157-169.

Diamond, I., Owolabi, T., Marco, M., Lam, C., and Glick, A. (2000). Conditional gene expression in the epidermis of transgenic mice using the tetracycline-regulated transactivators tTA and rTA linked to the keratin 5 promoter. J Invest Dermatol *115*, 788-794.

Grcevic, D., Pejda, S., Matthews, B.G., Repic, D., Wang, L., Li, H., Kronenberg, M.S., Jiang, X., Maye, P., Adams, D.J.*, et al.* (2012). In vivo fate mapping identifies mesenchymal progenitor cells. Stem cells (Dayton, Ohio) *30*, 187-196.

Parfitt, G.J. (2019). Immunofluorescence Tomography: High-resolution 3-D reconstruction by serial-sectioning of methacrylate embedded tissues and alignment of 2-D immunofluorescence images. Sci Rep *9*, 1992.

Richardson, A., Lobo, E.P., Delic, N.C., Myerscough, M.R., Lyons, J.G., Wakefield, D., and Di Girolamo, N. (2017). Keratin-14-Positive Precursor Cells Spawn a Population of Migratory Corneal Epithelia that Maintain Tissue Mass throughout Life. Stem Cell Reports *9*, 1081-1096.

Samokhvalov, I.M., Samokhvalova, N.I., and Nishikawa, S. (2007). Cell tracing shows the contribution of the yolk sac to adult haematopoiesis. Nature *446*, 1056-1061.

Zoukhri, D., Fix, A., Alroy, J., and Kublin, C.L. (2008). Mechanisms of murine lacrimal gland repair after experimentally induced inflammation. Invest Ophthalmol Vis Sci *49*, 4399-4406.